PHYSIOLOGY

Ca^{2+} concentration–dependent premature death of *igfbp5a*$^{-/-}$ fish reveals a critical role of IGF signaling in adaptive epithelial growth

Chengdong Liu[1,2]*, Yi Xin[1]*, Yan Bai[1], Grant Lewin[1], Gen He[2,3], Kangsen Mai[2,3], Cunming Duan[1†]

The phenotype gap is a challenge for genetically dissecting redundant endocrine signaling pathways, such as the six isoforms in the insulin-like growth factor binding protein (IGFBP) family. Although overexpressed IGFBPs can inhibit or potentiate IGF actions or have IGF-independent actions, mutant mice lacking IGFBP-encoding genes do not exhibit major phenotypes. We found that although zebrafish deficient in *igfbp5a* did not show overt phenotypes when raised in Ca^{2+}-rich solutions, they died prematurely in low Ca^{2+} conditions. A group of epithelial cells expressing *igfbp5a* take up Ca^{2+} and proliferate under low Ca^{2+} conditions because of activation of IGF signaling. Deletion of *igfbp5a* blunted low Ca^{2+} stress–induced IGF signaling and impaired adaptive proliferation. Reintroducing zebrafish Igfbp5a, but not its ligand binding–deficient mutant, restored adaptive proliferation. Similarly, adaptive proliferation was restored in zebrafish lacking *igfbp5a* by expression of human IGFBP5, but not two cancer-associated IGFBP5 mutants. Knockdown of IGFBP5 in human colon carcinoma cells resulted in reduced IGF-stimulated cell proliferation. These results reveal a conserved mechanism by which a locally expressed Igfbp regulates organismal Ca^{2+} homeostasis and survival by activating IGF signaling in epithelial cells and promoting their proliferation in Ca^{2+}-deficient states. These findings underscore the importance of physiological context when analyzing loss-of-function phenotypes of endocrine factors.

INTRODUCTION

Zebrafish live in hypo-osmotic environments and continuously lose Ca^{2+} and other ions into the surrounding water. They constantly take up Ca^{2+} from the aquatic habitat to maintain body fluid Ca^{2+} homeostasis. This vital task is accomplished by a group of epithelial cells called Na^+-K^+-ATPase–rich (NaR) cells in zebrafish (*1*). NaR cells are functionally equivalent to human intestinal epithelial cells, and they contain all major molecular components of the transcellular Ca^{2+} transport machinery, including the epithelial calcium channel Trpv5/6 (*1*, *2*). Although distributed in the adult intestine and gills (a major osmoregulatory organ in fish), NaR cells are located on the yolk sac skin during the embryonic and larval stages, making them easily accessible for experimental manipulation and observation (*1*, *3*, *4*). When faced with low-[Ca^{2+}] challenge, preexisting NaR cells reenter the cell cycle to yield more cells (*3*, *4*). This is considered to be an adaptive response that allows fish to acquire adequate Ca^{2+} to keep their body fluid [Ca^{2+}] constant to survive under low-[Ca^{2+}] environments (*3*, *4*). Ca^{2+} deficiency also stimulates the proliferation of mammalian and human intestinal epithelial cells (*5*–*8*), suggesting an evolutionarily conserved mechanism. We have shown that low-[Ca^{2+}] stress activates insulin-like growth factor (IGF) receptor (IGF1R)–mediated phosphoinositide 3 kinase (PI3K)–Akt–target of rapamycin (Tor) signaling specifically in NaR cells and the increased IGF signaling promotes NaR cells to reenter the cell cycle and proliferate (*3*, *4*). How the IGF signaling is activated specifically in NaR cells under low-[Ca^{2+}] stress is not fully understood.

IGFs are evolutionarily ancient polypeptides structurally related to insulin. IGF binds to and activates the IGF1R, a receptor tyrosine kinase that is structurally related to the insulin receptor. Unlike insulin, however, IGFs are bound to one of six types of IGF binding proteins (IGFBPs) in extracellular fluids. Binding to an IGFBP increases the half-life of IGF in the circulation and prevents the potential interaction of IGFs to the insulin receptor (*9*, *10*). In addition to these endocrine roles, gain-of-function studies have suggested that IGFBPs can also act locally, both negatively and positively modulating IGF action in target tissues; in addition, some IGFBPs have IGF-independent biological activities (*9*–*12*). Some IGFBPs are present in the nucleus and have nuclear activity (*12*). Unexpectedly, mice lacking IGFBP-encoding genes do not exhibit major phenotypes. *IGFBP2* knockout mice are phenotypically normal with the exception of minor gender-specific changes in bone structure and minor changes in the spleen and liver in adult males (*13*, *14*). *IGFBP3* knockout mice are normal in size (*15*). Deletion of the *IGFBP4* gene in mice results in a mild 10 to 15% reduction in prenatal growth, which is somewhat paradoxical given that overexpression of IGFBP4 also reduces growth (*15*). *IGFBP5* knockout mice are phenotypically normal (*15*). The *IGFBP3*, *IGFBP4*, and *IGFBP5* triple knockout mice are viable and only show a 25% reduction in body growth (*15*). The mechanisms underlying the lack of phenotypes are poorly understood.

We have previously reported that a zebrafish *igfbp* gene, *igfbp5a*, is specifically expressed in NaR cells (*3*). Knockdown of Igfbp5a using antisense morpholinos decreases the low-[Ca^{2+}] stress–induced Akt signaling, suggesting that locally expressed Igfbp5a may be important (*3*). Because morpholinos only knock down target genes transiently, this approach could not be used to investigate the possible role of Igfbp5a in adaptive NaR cell proliferation nor the long-term biological consequence. Furthermore, we now understand that morpholinos have many limitations, including high toxicity and "off-target" effects (*16*). Here, we sought to investigate the functional role of Igfbp5a in NaR cells and its long-term functional role by deleting Igfbp5a with TALEN (transcription activator-like effector nuclease) and CRISPR-Cas9 (clustered regularly interspaced short palindromic repeats–CRISPR-associated 9)

[1]Department of Molecular, Cellular and Developmental Biology, University of Michigan, Ann Arbor, MI 48109, USA. [2]The Key Laboratory of Mariculture, Education Ministry of China and College of Fisheries, Ocean University of China, Qingdao 266003, China. [3]Pilot National Laboratory for Marine Science and Technology (Qingdao), Qingdao 266237, China.
*These authors contributed equally to this work
†Corresponding author. Email: cduan@umich.edu

technology. The *igfbp5a*$^{-/-}$ mutant fish appeared indistinguishable from their wild-type siblings when raised in Ca^{2+}-rich embryo solutions. When raised in regular water or low Ca^{2+} solutions, however, they died prematurely. Further analyses showed that deletion of Igfbp5a impaired the low-[Ca^{2+}] stress–induced NaR cell proliferation and diminished IGF signaling. The diminished IGF signaling and NaR cell proliferation were restored by reintroducing Igfbp5a or human IGFBP5. Further analyses suggested that Igfbp5a acts by binding to IGF ligand and activating Akt-Tor signaling in epithelial cells under Ca^{2+}-deficient states and that this action is conserved in human colon cells.

RESULTS

Two independent F_1 lines were obtained using a TALEN-based approach (Fig. 1A and fig. S1, A and B). Both are predicted to be null alleles. The *igfbp5aΔ4* line harbors a 4–base pair (bp) deletion allele that introduces a 23–amino acid sequence shortly after the signal peptide. The *igfbp5aΔ11* line contains an 11-bp deletion allele, which truncates Igfbp5a after the signal peptide. F_2 progeny from these lines were raised in the standard embryo solution (containing 0.33 mM [Ca^{2+}] and referred to as E3 solution hereafter) to 5 days postfertilization (dpf) and transferred to the standard fish system water. Genotyping of adults showed a complete lack of homozygous adult fish in both lines. To determine whether the mutant fish died prematurely, we intercrossed each of the two F_1 lines and randomly genotyped their F_2 progeny at the larval and adult stages. Whereas 27% of larvae (5 dpf) in the *igfbp5aΔ4* group were homozygous, adult progeny were either heterozygous or wild-type (Fig. 1B). Similarly, none of homozygous *igfbp5aΔ11* fish (20% detected at 3 dpf) survived to 3 months (Fig. 1B). Among the survived *igfbp5aΔ11* adult fish, 43% were heterozygous (Fig. 1B).

Because *igfbp5a* mRNA is specifically expressed in NaR cells, which are crucial for Ca^{2+} uptake, we speculated that the mutant fish died because of deficiency of this essential ion. If this notion were correct, then raising the progeny in embryo solutions containing high [Ca^{2+}] should rescue the mutant fish because Ca^{2+} can enter through paracellular transport. When progeny of *igfbp5aΔ4* intercrosses and *igfbp5aΔ11* intercrosses were raised in 5PPT solution (containing

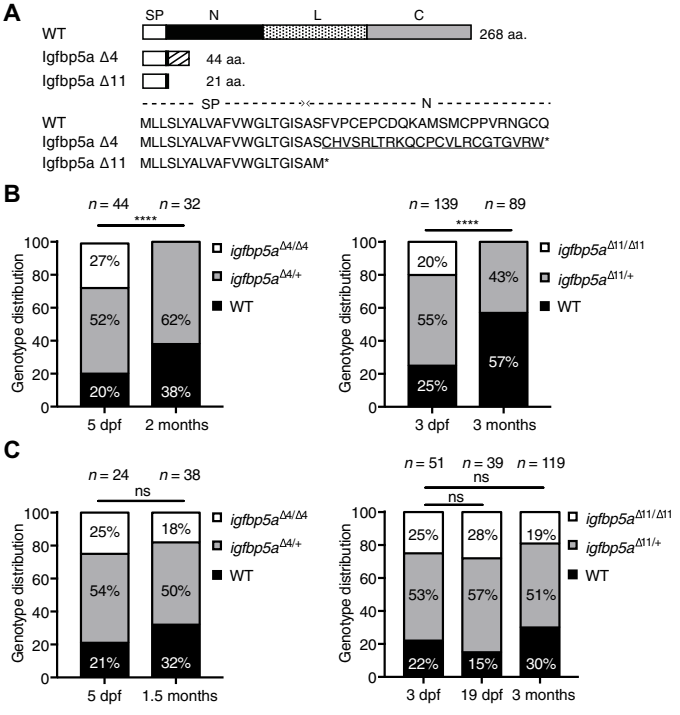

Fig. 1. Deletion of Igfbp5a leads to premature death. (**A**) Structure of wild-type (WT) Igfbp5a, Igfbp5aΔ4, and Igfbp5aΔ11. SP, signal peptide. N, L, and C indicate the N-, L-, and C-domain of Igfbp5a. Asterisk (*) indicates a stop codon. The underlined amino acids were introduced by a frameshift. aa, amino acids. (**B** and **C**) F_2 progeny of *igfbp5aΔ4*$^{+/-}$ intercrosses (left panel) and *igfbp5aΔ11*$^{+/-}$ (right panel) intercrosses were raised in E3 solution until 3 or 5 dpf and transferred into either fish system water (B) or 5PPT high [Ca^{2+}] solution (C). The fish were sampled randomly and genotyped at the indicated stages. The genotype distributions are shown. ****$P < 0.0001$ by χ^2 test. ns, not statistically significant. Total number of fish in each group is shown above the bar.

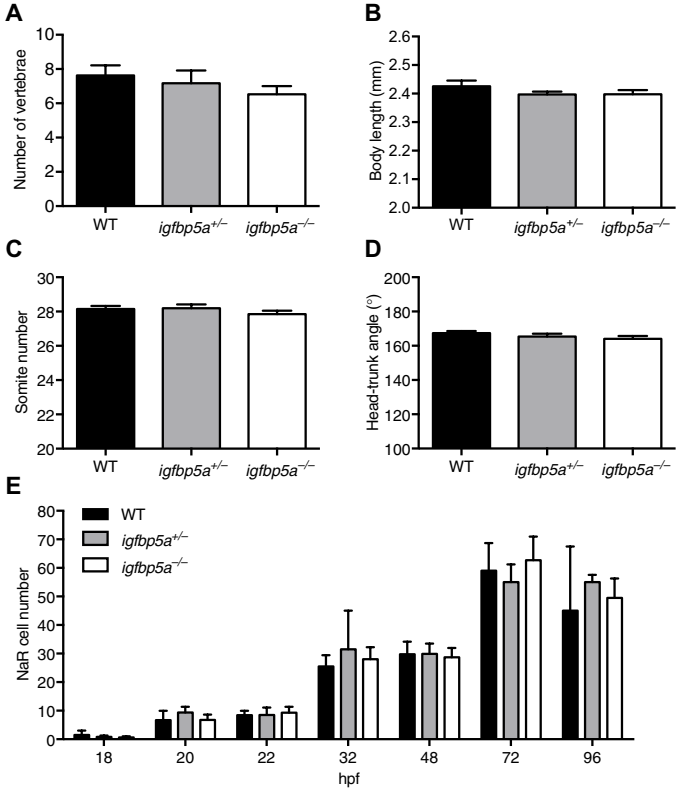

Fig. 2. *igfbp5a*$^{-/-}$ mutant fish develop and grow normally in Ca^{2+}-rich solutions. (**A**) Progeny of *igfbp5a*$^{+/-}$ intercrosses were raised in E3 solution until 5 dpf and transferred into high [Ca^{2+}] 5PPT solution. The vertebrate columns of 12 dpf larvae were visualized by calcein staining and quantified. Data shown are means ± SEM. $n = 18$ to 19 fish per group. No statistically significant differences were found among the groups using one-way analysis of variance (ANOVA), followed by Tukey's multiple comparison test. (**B** to **D**) Embryos of the indicated genotypes were raised in E3 solution. Their body length (B) and somite number (C) were measured at 24 hours postfertilization (hpf), and head-trunk angle (D) was measured at 72 hpf. Data shown are means ± SEM. $n = 12$ to 73 fish per group. No statistically significant differences were found using one-way ANOVA, followed by Tukey's multiple comparison test. (**E**) Progeny of *igfbp5a*$^{+/-}$ intercrosses were sampled at the indicated stages. After NaR cells were visualized by in situ hybridization using a *trpv5/6* complementary RNA (cRNA) probe and quantified, the fish were genotyped individually. Data shown are means ± SEM. $n = 6$ to 14 fish per group. No statistically significant differences were found by one-way ANOVA, followed by Tukey's multiple comparison test.

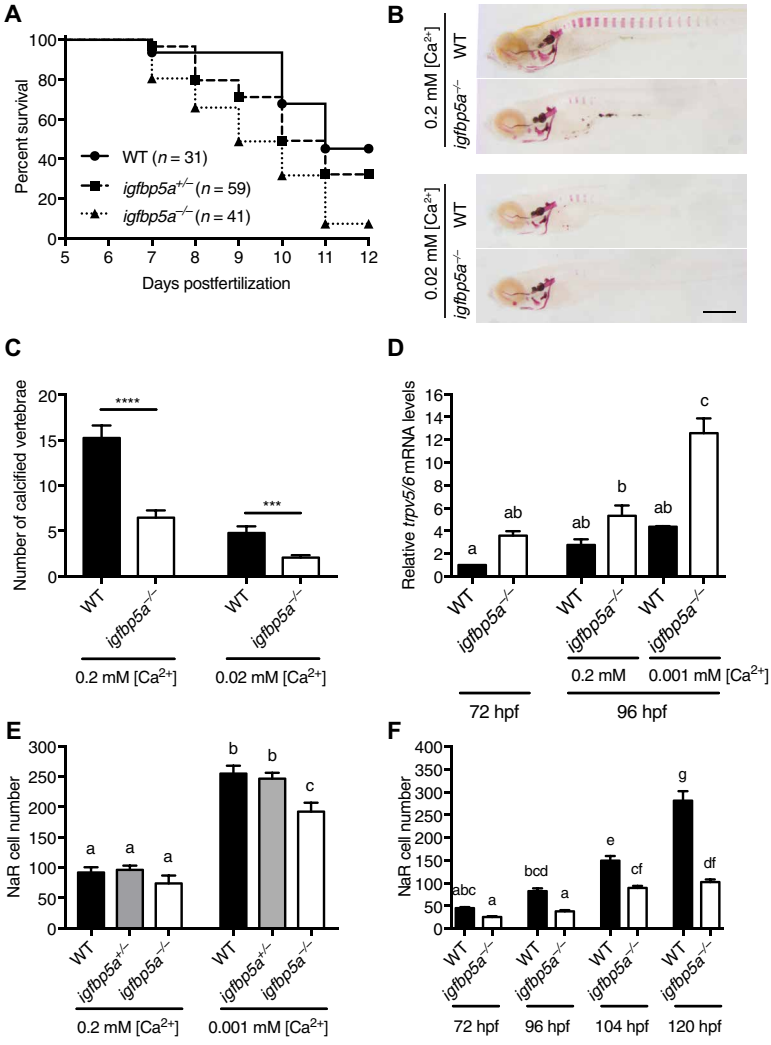

Fig. 3. Deletion of Igfbp5a increases mortality and impairs adaptive NaR cell proliferation. (**A**) Progeny of *igfbp5a*$^{+/-}$ intercrosses were raised in E3 solution until 5 dpf and transferred into low-[Ca^{2+}] solution. Dead larvae were collected daily and genotyped. The survival curve is shown, and the numbers of fish are indicated. $P < 0.0001$ by log-rank test. (**B** and **C**) Fish of the indicated genotypes were raised in solutions containing the indicated Ca^{2+} concentration to 11 dpf and stained by Alizarin red. Representative images are shown in (B), and the average number of calcified vertebral columns is shown in (C). $n = 19$ to 29 fish per group. ***$P < 0.001$, ****$P < 0.0001$, unpaired two-tailed t test. Scale bar, 0.5 mm. (**D**) Embryos of the indicated genotypes were raised in E3 solution until 72 hpf and transferred to solutions containing the indicated Ca^{2+} concentration. The expression of *trpv5/6* mRNA was measured by quantitative polymerase chain reaction (qPCR) and normalized to the NaR cell number for the group. Values are means ± SEM of three independent experiments, each containing RNA isolated from a pool of 20 larvae of the indicated stages. Different letters indicate statistically significant differences ($P < 0.05$ by one-way ANOVA, followed by Tukey's multiple comparison test). (**E**) Progeny of *igfbp5a*$^{+/-}$ intercrosses were raised in E3 solution to 72 hpf and transferred to solutions containing the indicated Ca^{2+} concentration. The fish were sampled at 120 hpf. NaR cells were visualized by in situ hybridization using the *trpv5/6* cRNA probe and quantified. Each larva was genotyped afterward. Data shown are means ± SEM. $n = 13$ to 40 fish per group. Different letters indicate statistically significant differences ($P < 0.05$ by one-way ANOVA, followed by Tukey's multiple comparison test). (**F**) *Tg(igfbp5a:GFP)* fish of the indicated genotypes were raised in E3 solution until 72 hpf and transferred to low-[Ca^{2+}] solution. The number of GFP-labeled NaR cells was quantified at 72, 96, 104, and 120 hpf. Data shown are means ± SEM. $n = 7$ to 36 fish per group. Different letters indicate statistically significant differences ($P < 0.05$ by one-way ANOVA, followed by Tukey's multiple comparison test).

1.6 mM [Ca^{2+}] and referred to as high [Ca^{2+}] solution hereafter), many mutant fish grew to adulthood (Fig. 1C). The adult mutant fish in both lines were fertile and morphologically indistinguishable from their siblings. There were no notable differences in the growth rate or speed of development (Fig. 2, A to D). The *igfbp5aΔ11* line, referred to as *igfbp5a*$^{-/-}$ mutant fish hereafter, was used in subsequent studies unless otherwise stated.

To investigate whether Igfbp5a plays a local role in NaR cell development, we randomly sampled progeny from an *igfbp5a*$^{+/-}$ intercross at various stages. NaR cells were visualized and quantified, and each fish was genotyped individually. There was no difference in the NaR cell number between the *igfbp5a*$^{-/-}$ mutants and their siblings at all stages examined (Fig. 2E). A heteroduplex mobility assay (HMA) confirmed the expression of *igfbp5aΔ11* mutant mRNA in *igfbp5a*$^{-/-}$ mutants (fig. S2A). The expression of *igfbp5a* was similar between *igfbp5a*$^{-/-}$ mutant fish and their siblings (fig. S2B), suggesting that nonsense-mediated decay of *igfbp5a* mRNA did not occur. Furthermore, the expression pattern (fig. S3, A and B) and mRNA levels (fig. S3C) of the paralogous *igfbp5b* were also similar between wild-type and *igfbp5a*$^{-/-}$ mutant fish. Finally, low-[Ca^{2+}] treatment did not change *igfbp5b* mRNA levels in either wild-type or *igfbp5a*$^{-/-}$ mutant fish (fig. S3D).

To confirm that *igfbp5a*$^{-/-}$ fish were prone to premature death, we performed a low-[Ca^{2+}] challenge test with 5-dpf larvae obtained from an *igfbp5a*$^{+/-}$ intercross. *igfbp5a*$^{-/-}$ mutant fish died earlier and at a significantly greater rate (Fig. 3A). On 2 and 3 days after the low-[Ca^{2+}] challenge, *igfbp5a*$^{-/-}$ mutants comprised 66 and 38% of the dead larvae. These values were much greater than the expected 25% according to Mendelian ratio. Similarly, *igfbp5aΔ4* mutant fish died at a significantly greater rate under the low-[Ca^{2+}] challenge (fig. S4). We hypothesized that the premature death of *igfbp5a*$^{-/-}$ fish was due to Ca^{2+} deficiency in the body. Alizarin red staining showed that calcified bone mass in mutant fish raised in a solution containing 0.2 mM [Ca^{2+}] (referred to as regular [Ca^{2+}] solution hereafter because its [Ca^{2+}] is similar to fish system water) was comparable to that of wild-type fish raised in a solution with 10-fold lower Ca^{2+} levels (Fig. 3B). Calcified bone mass in *igfbp5a*$^{-/-}$ fish was further reduced by exposure to the lower [Ca^{2+}] solution (Fig. 3, B and C). Increased expression of *trpv5/6*, which encodes a channel that fluxes cations including Ca^{2+}, is a hallmark of body calcium deficiency (*1*, *4*). *igfbp5a*$^{-/-}$ mutants had increased *trpv5/6* expression in NaR cells when raised in regular [Ca^{2+}] solution (Fig. 3D). Low-[Ca^{2+}] challenge

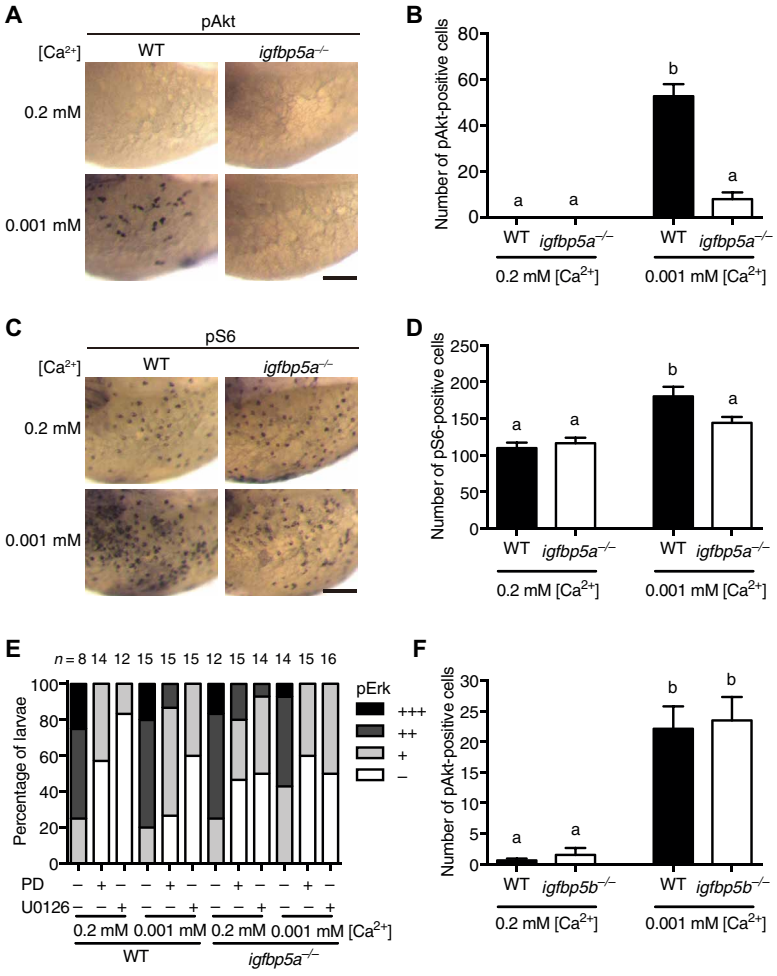

Fig. 4. Deletion of Igfbp5a but not its paralog Igfbp5b impairs low-[Ca^{2+}] stress–induced Akt-Tor signaling in NaR cells. (**A** to **D**) Fish of the indicated genotypes raised in E3 solution were transferred to solutions containing the indicated Ca^{2+} concentration at 72 hpf. After 24 hours, they were stained for phosphorylated Akt (pAkt) (A and B) or phosphorylated S6 (pS6) (C and D). Representative images are shown in (A) and (C). Scale bar, 0.1 mm. The numbers of cells positive for phosphorylated Akt or phosphorylated S6 in each fish were quantified, and the quantitative results are shown in (B) and (D). Values are means ± SEM. n = 6 to 12 fish per group. Different letters indicate statistically significant differences between groups ($P < 0.05$ by one-way ANOVA, followed by Tukey's multiple comparison test). (**E**) Fish of the indicated genotypes were raised in E3 solution to 72 hpf and transferred to solutions containing the indicated [Ca^{2+}] with or without U0126 (10 μM) or PD98059 (10 μM). After 8 hours, they were stained for phosphorylated Erk (pErk). The phosphorylated Erk signal was scored following a previously published scoring system (*3*). Total numbers of fish are shown above the bar. (**F**) Larvae of the indicated genotypes were raised in E3 solution to 72 hpf and transferred to solutions containing the indicated Ca^{2+} concentration. After 8 hours, they were stained for phosphorylated Akt. The number of cells positive for phosphorylated Akt was quantified. Values are means ± SEM. n = 13 to 18 fish per group. Different letters indicate statistically significant differences ($P < 0.05$ by one-way ANOVA, followed by Tukey's multiple comparison test).

treatment increased *trpv5/6* mRNA levels in both wild-type and *igfbp5a*$^{-/-}$ fish, but the magnitude of increase was greater in *igfbp5a*$^{-/-}$ fish. These results suggest that deletion of Igfbp5a leads to body Ca^{2+} deficiency, and low-[Ca^{2+}] treatment further exacerbates the Ca^{2+} deficiency.

When acclimated to low-[Ca^{2+}] environments, NaR cells undergo proliferation to yield more NaR cells to ensure sufficient Ca^{2+} uptake for survival (*3*, *4*). We tested whether deletion of Igfbp5a impaired this adaptive proliferation response. Visualization of NaR cells by in situ hybridization using a *trpv5/6* probe showed that 48 hours of low-[Ca^{2+}] treatment significantly increased the NaR cell number in wild-type and heterozygous larvae, an increase that was blunted in *igfbp5a*$^{-/-}$ larvae (Fig. 3E). We next crossed *igfbp5a*$^{-/-}$ fish with *Tg(igfbp5a:GFP)* fish, a transgenic line in which NaR cells are labeled by green fluorescent protein (GFP) expression, allowing real-time visualization and quantification of NaR cell division (*4*). Low-[Ca^{2+}] treatment resulted in significant increases in NaR cells in *Tg(igfbp5a:GFP)* larvae at 96, 104, and 120 hpf (Fig. 3F). This increase was significantly reduced in *igfbp5a*$^{-/-}$*;Tg(igfbp5a:GFP)* larvae (Fig. 3F). Next, we performed transient knockout experiments in *Tg(igfbp5a:GFP)* fish using a CRISPR-Cas9–based approach (fig. S5A). Transient deletion of Igfbp5a using two different synthetic guide RNAs (sgRNAs) significantly decreased NaR cell proliferation under low-[Ca^{2+}], but not under normal [Ca^{2+}] (fig. S5B). Therefore, either permanent or transient deletion of Igfbp5a impairs the adaptive proliferation response of NaR cells.

RNA expression analysis showed that among members of the IGF and insulin gene family, *igf2b* was most abundantly expressed in NaR cells, followed by *igf2a* (fig. S6A). The expression of *igf1*, *igf3* (also known as *igf1b*), *insulin a*, and *insulin b* was minimal (fig. S6A). The strong expression of *igf2b* mRNA in NaR cells was confirmed by in situ hybridization analysis of *Tg(igfbp5a:GFP)* larvae (fig. S6B). The two *igf1r* genes and two *insr* genes were all expressed in NaR cells with *igf1ra* being the most abundant (fig. S6A). Low-[Ca^{2+}] treatment did not alter the expression of these genes (fig. S6, A and B).

Our previous studies have shown that low-[Ca^{2+}] treatment induces the phosphorylation of Akt exclusively in NaR cells (*3*, *4*). Accordingly, immunostaining analysis revealed that there were few phosphorylated Akt–positive NaR cells on the yolk sac in wild-type larvae under regular [Ca^{2+}] conditions. Low-[Ca^{2+}] treatment resulted in a robust increase in NaR cells positive for phosphorylated Akt (Fig. 4, A and B). In comparison, low-[Ca^{2+}] treatment resulted in significantly fewer NaR cells that were positive for phosphorylated Akt in *igfbp5a*$^{-/-}$ larvae (Fig. 4, A and B), suggesting that deletion of Igfbp5a impairs Akt signaling in NaR cells. Similar results were observed with phosphorylated S6, an indicator of Tor signaling, although basal phosphorylated S6 levels were higher (Fig. 4, C and D). In contrast, phosphorylated Erk levels were similar between wild-type and *igfbp5a*$^{-/-}$ larvae under both

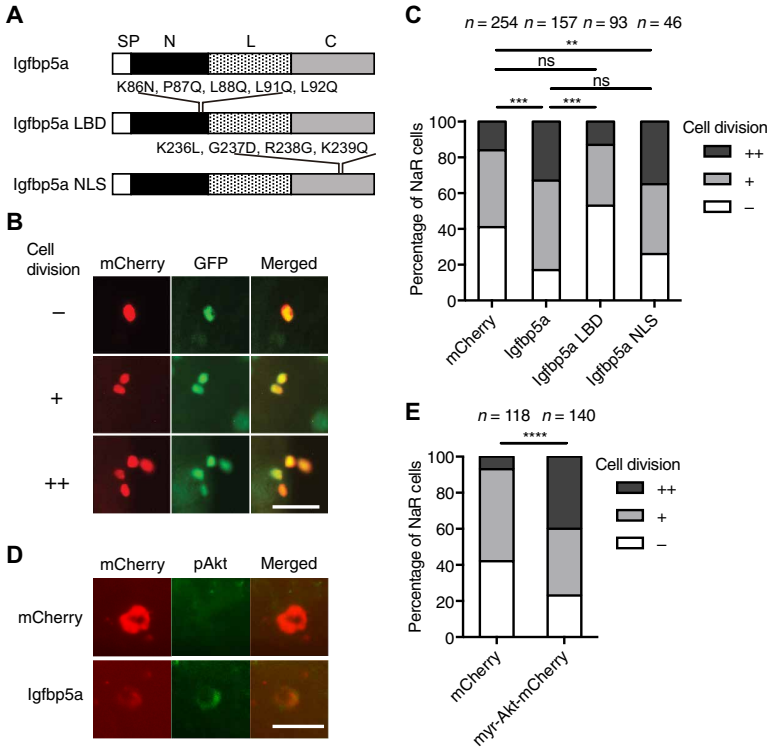

Fig. 5. Reintroduction of Igfbp5a or constitutively active Akt in NaR cells restores adaptive proliferation. (**A**) Structure of zebrafish Igfbp5a and its mutants. SP, N-, L-, and C-domains are indicated. Mutated residues are shown. (**B** and **C**) NaR division scoring system. Zebrafish *igfbp5a*$^{-/-}$*;Tg(igfbp5a:GFP)* embryos injected with BAC(*igfbp5a:Igfbp5a-IRES-mCherry)* constructs containing the indicated genes were raised in E3 solution until 72 hpf and transferred to low-[Ca^{2+}] solutions. Igfbp5a-expressing NaR cells are labeled by both GFP and mCherry. The NaR division scoring system is shown in (B). During the 48-hour treatment period, NaR cells that divide 0, 1, or 2 times were scored as –, +, and ++. Scale bar, 0.05 mm. The quantified data are shown in (C). χ^2 test was used for statistical analysis. $^{**}P < 0.01$, $^{***}P < 0.001$. Total numbers of cells are shown above the bar. (**D**) The larvae described in (B) and (C) were collected after 24 hours in low-[Ca^{2+}] solution and stained for phosphorylated Akt and mCherry. Scale bar, 0.02 mm. (**E**) BAC(*igfbp5a:myr-Akt-mCherry)* DNA was injected into *igfbp5a*$^{-/-}$*;Tg(igfbp5a:GFP)* embryos. NaR division was scored as described in (B). χ^2 test was used for statistical analysis. $^{****}P < 0.0001$. Total numbers of cells are shown above the bar.

regular and low-[Ca^{2+}] conditions (Fig. 4E and fig. S7). The phosphorylated Erk signal was authentic because it was abolished by MAPK (mitogen-activated protein kinase) kinase (MEK) inhibitor treatment (Fig. 4E and fig. S7). Deletion of the paralogous *igfbp5b* gene using CRISPR-Cas9 did not change the induction of phosphorylated Akt in NaR cells by low-[Ca^{2+}] treatment (Fig. 4F).

To test whether expression of Igfbp5a was sufficient to activate IGF signaling in NaR cells, we randomly expressed zebrafish Igfbp5a, its ligand binding domain (LBD), or nuclear localization signal (NLS) mutants in NaR cells in *igfbp5a*$^{-/-}$*;Tg(igfbp5a:GFP)* larvae using a Tol2 transposon bacterial artificial chromosome (BAC)–mediated genetic mosaic assay (Fig. 5, A and B). NaR cells expressing Igfbp5a proliferated under low-[Ca^{2+}] stress and were positive for phosphorylated Akt (Fig. 5, C and D). NaR cell proliferation in *igfbp5a*$^{-/-}$*;Tg(igfbp5a:GFP)* larvae under low-[Ca^{2+}] stress was also restored by the expression of the Igfbp5a NLS mutant, but not by that of the LBD mutant (Fig. 5C), suggesting that Igfbp5a acts in an IGF binding–dependent manner. If Igfbp5a indeed stimulates NaR cell proliferation by binding to IGFs and activating Akt signaling, then expression of a constitutively active Akt should rescue the defective NaR cell proliferation in *igfbp5a*$^{-/-}$ larvae. Expression of myr-Akt restored NaR cell proliferation in response to low-[Ca^{2+}] stress (Fig. 5, D and E). This approach does not rescue the lethality phenotype, presumably because it targets Igfbp5a expression transiently only in a small number of NaR cells.

To test whether IGFBP5 acts in a similar manner in human epithelial cells, human colon carcinoma (LoVo) cells were transfected with a validated small interfering RNA (siRNA) plasmid (pSuperBP5) targeting human IGFBP5 L-domain (*17*). In cells transfected with the empty pSuper plasmid, IGF2 treatment resulted in a significant increase in the percentage of S-phase cells. This increase was abolished in the pSuperBP5 transfected cells (Fig. 6A), suggesting that the endogenous IGFBP5 is required in the proliferative response of these human cells to IGF2 stimulation. To demonstrate the specificity of the siRNA knockdown effect and the sufficiency of IGFBP5, we cotransfected LoVo cells with pSuperBP5 and IGFBP545, which is not targeted by pSuperBP5 because it contains the IGFBP5 N- and C-domain but the L-domain from IGFBP4 (*17*). Expression of IGFBP545 restored the proliferation response to IGF2 stimulation (Fig. 6A). To further investigate the function of human IGFBP5 and its mechanism of action in an in vivo setting, we expressed human IGFBP5 and two mutants (G223R and W242*) in NaR cells in *igfbp5a*$^{-/-}$*;Tg(igfbp5a:GFP)* embryos using the Tol2 transposon BAC genetic mosaic assay (Fig. 6B). G223R and W242* are two cancer-associated mutations that have been speculated to have lost IGF binding ability (*18*). Ectopic expression of wild-type human IGFBP5, but not these mutants, significantly increased NaR cell proliferation under low-[Ca^{2+}] stress (Fig. 6C). These results suggest that human IGFBP5 acts by binding to the IGF ligand and promoting IGF action in human LoVo cells.

DISCUSSION

IGFBP5 is the most conserved member of the IGFBP family (*11*, *12*) and has been reported to inhibit or potentiate IGF or acts as a growth factor itself in mammalian cells (*9*–*12*). Despite these findings, *IGFBP5*-deficient mice do not have overt phenotypes (*19*). Here, we showed that genetic deletion of zebrafish Igfbp5a causes body Ca^{2+} deficiency and premature death under regular laboratory conditions. The *igfbp5a*$^{-/-}$ mutant larvae exhibited clear and specific defects in NaR cell adaptive proliferation under Ca^{2+}-deficient conditions. These results reveal a critical role of Igfbp5a in regulating organismal survival and calcium balance by promoting NaR cell proliferation under low-calcium states.

The lack of phenotype in *IGFBP5*-null or other *IGFBP*-null mice has been postulated to be due to the genetic redundancy in the

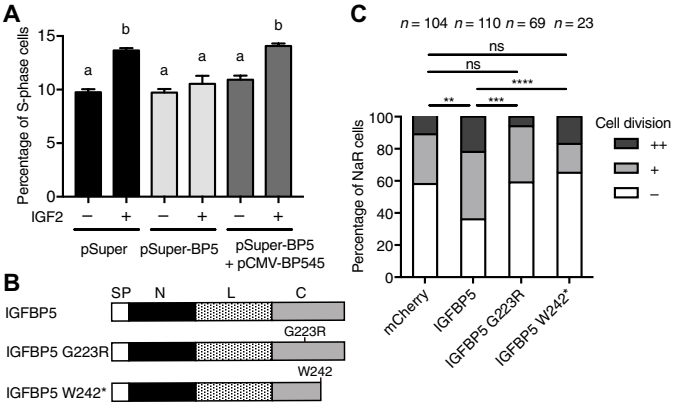

Fig. 6. IGFBP5 but not two cancer-associated IGFBP5 mutants promotes the mitotic response of human epithelial cells to IGF stimulation. (**A**) Human LoVo epithelial cells were transfected with the indicated siRNA construct with or without pCMV-BP545. After 24 hours, they were treated with human IGF2 (400 ng/ml) for 3 days and analyzed by flow cytometry. The percentage of S-phase cells is shown. Values shown are means ± SEM. $n = 3$ independent experiments. Groups labeled with different letters are statistically significantly different from each other ($P < 0.05$ by one-way ANOVA, followed by Tukey's multiple comparison test). (**B**) Structure of human IGFBP5 and its two cancer-associated mutants. SP, N-, L-, and C-domains are indicated. Mutated residues are shown. Asterisk (*) indicates a stop codon. (**C**) Zebrafish *igfbp5a*$^{-/-}$*;Tg(igfbp5a:GFP)* embryos injected with the indicated human IGFBP5 construct were raised in E3 solution until 72 hpf and transferred to low-[Ca^{2+}] solution. Forty-eight hours later, GFP and mCherry double-positive cells were quantified using the scoring system shown in Fig.5B. χ^2 test was used for statistical analysis. **$P < 0.01$, ***$P < 0.001$, ****$P < 0.001$. Total numbers of cells are shown above the bar.

mouse model (*12*). The use of CRISPR-Cas9 and TALEN to delete and edit genes suggest that the phenotype gap is also present in zebrafish. Many cases have been reported in which permanent deletion of gene(s)-encoding various hormones and growth factors, including many that were previously thought to be critical or even essential, does not result in notable phenotypic changes (*16*, *20*–*23*). Genetic studies in zebrafish have also found major discrepancies in phenotypes between permanent knockout and transient knockdowns (*24*–*27*). Several additional mechanisms, including genetic compensation and/or transcriptional adaptation, nonsense-mediated decay, and altered mRNA processing, have been proposed to account for the lack of phenotypes in permanent genetic mutants (*16*, *27*). These mechanisms cannot fully explain the findings of this study. Because the zebrafish genome contains nine *igfbp* genes due to a teleost-specific genome-wide duplication event (*28*), one could argue that zebrafish may have a greater genetic redundancy than mice. For example, there are two *igfbp5* genes in zebrafish compared to a single *IGFBP5* gene in mice and humans (*29*). Nevertheless, our genetic data showed that permanent deletion of Igfbp5a compromised the adaptive NaR cell proliferation response and led to low body Ca^{2+} content and premature death. We did not detect nonsense-mediated mRNA decay of *igfbp5a* mRNA or observe compensatory increases in the paralogous *igfbp5b* expression in the *igfbp5a*$^{-/-}$ mutant fish. Furthermore, transient deletion of Igfbp5a resulted in similar defects in NaR cells. The phenotypes of the *igfbp5a*$^{-/-}$ mutant fish were context-dependent. When raised in [Ca^{2+}]-rich solutions, *igfbp5a*$^{-/-}$ mutant fish grew to the adult stage and appeared indistinguishable from their siblings. However, when raised in low-[Ca^{2+}] solutions, they showed specific defects in adaptive NaR cell proliferation and died prematurely. These context-dependent phenotypes were specific because these changes were not found in *igfbp5b*$^{-/-}$ mutant fish. Our findings underscore the importance of physiological context in genetic dissection of the highly redundant endocrine signaling network.

In addition to regulating global growth and development (*30*, *31*), IGF signaling also exerts many cell type–specific and context-dependent actions (*11*, *23*). How the IGF signaling system exerts these cell type–specific and context-dependent actions is not well understood. Here, we showed that genetic deletion of Igfbp5a, but not the closely related Igfbp5b, reduced IGF1R-mediated Akt and Tor signaling specifically in NaR cells and in a Ca^{2+} concentration–dependent manner. Reintroducing Igfbp5a was sufficient to activate Akt signaling in mutant NaR cells and restore their proliferation. Moreover, knockdown of IGFBP5 abolished the proliferation of human LoVo cells in response to IGF2 stimulation, an effect that was rescued by expression of a siRNA-resistant form of IGFBP5. These results reveal a conserved mechanism by which a locally expressed IGFBP activates the IGF signaling in a cell type–specific and context-dependent manner.

IGFBP5 appears to have several modes of actions. When added to cultured human or rodent cells together with IGF1 or IGF2, IGFBP5 inhibits IGF-induced cell proliferation and/or differentiation (*18*, *29*, *32*–*34*). IGFBP5 can also potentiate IGF-induced cell proliferation and/or survival (*35*–*39*). IGFBP5 also has IGF-independent activities (*10*–*12*). Mammalian IGFBP5 is detected in the nucleus and has nuclear activity (*40*, *41*), properties also observed in zebrafish (*29*). How IGFBP5 acts in vivo under a physiological context has not been reported. Here, we found that Igfbp5a acted by binding to IGF and activating Akt-Tor signaling in NaR cells and that nuclear localization is not important for this action of Igfbp5a. Our gene expression analysis indicated that both *igf1r* genes were detected in NaR cells with *igf1ra* being the more abundant isoform. Future studies will be needed to determine whether Igfbp5 acts by binding to Igf2b to activate Igf1ra and/or Igf1rb in NaR cells. Mammalian cell culture and biochemical studies suggest that IGFBP5 can potentiate IGF action by bringing IGF to the IGF1R through the proteolysis of IGFBP5 or through association with the cellular membrane or extracellular matrix proteins (*37*, *42*, *43*). Whether these mechanisms are involved in Igfbp5a action in NaR cells need to be elucidated with future studies.

Aberrant regulation or mutations of key components in the IGF-PI3K-AKT-TOR signaling pathway have been linked to major human diseases including cancers (*44*). In colon cancers, for example, several genes belonging to this pathway are mutated (*45*). These mutations result in increased *IGF2* expression, increased PIK3CA and PIK3R1 activity, and reduced *PTEN* expression or activity (*46*). Ding *et al.* (*18*) have identified more than 20 nonsynonymous mutations for IGFBP5 in cancer, including several frameshift and nonsense mutations. Because the IGF-PI3K-Akt-Tor pathway is highly conserved and activation of this pathway is both required and sufficient for NaR cell proliferation, the zebrafish larvae–NaR cell system provides an excellent in vivo platform for functional analysis of these cancer-associated mutations. As a proof-of principle experiment, we assessed two cancer-associated IGFBP5 mutants, G223R and W242*. Unlike wild-type IGFBP5, neither mutant could stimulate NaR cell proliferation in vivo. These results provided in vivo evidence supporting the idea that IGFBP5 G223R and W242* have lost IGF binding ability (*18*).

In summary, the findings in this study reveal a conserved mechanism by which a locally expressed Igfbp regulates organismal Ca^{2+}

homeostasis and survival by activating IGF signaling in epithelial cells and promoting their proliferation under Ca^{2+}-deficient states. This regulatory mechanism may not be limited to zebrafish or IGFBP5. Although IGFBP5 knockout mice exhibit normal mammary gland development under normal conditions, these animals show delayed mammary gland involution and enhanced alveolar bud formation after ovariectomy, followed by estrogen treatment (*19*). In breast cancer cells, doxorubicin-induced senescence increases IGFBP3 expression and cleavage of IGFBP3 prevents cell senescence (*9*). In human vascular endothelial cells, hypoxia induces the expression of IGFBP6, which in turn suppresses angiogenesis as a negative feedback during tumor growth (*47*). Future studies are needed to identify additional stress or disease conditions to which different IGFBPs respond to and to determine whether regulation of IGF signaling locally by IGFBPs is a widespread mechanism.

MATERIALS AND METHODS

Ethics statement

All experiments were conducted in accordance with the guidelines approved by the Institutional Committee on the Use and Care of Animals, University of Michigan.

Zebrafish husbandry and embryo rearing media with different Ca^{2+} concentrations

All zebrafish lines were raised and crossed according to zebrafish husbandry guidelines (*48*). Embryos were obtained by natural cross and staged according to Kimmel *et al.* (*49*). Several embryo rearing media were used. A standard solution containing 0.33 mM [Ca^{2+}], referred to as E3 solution, was prepared as described in *The Zebrafish Book: A Guide for the Laboratory Use of Zebrafish (Danio rerio)* (*48*). A solution containing high concentration of Ca^{2+} (1.6 mM [Ca^{2+}]), referred to as 5PPT high [Ca^{2+}] solution, was prepared by dissolving 5 g of Instant Ocean salt in 1000 ml of distilled water. Two embryo rearing solutions containing either 0.2 mM [Ca^{2+}] (referred to as regular [Ca^{2+}] solution) or 0.001 mM [Ca^{2+}] (referred to as low-[Ca^{2+}] solution) were prepared as previously reported (*3*). To inhibit pigmentation, 0.003% (w/v) *N*-phenylthiourea was added to these solutions.

Chemicals and reagents

Reagents were purchased from Thermo Fisher Scientific unless stated otherwise. The MEK inhibitors (U0126 and PD98059), phospho-Akt, phospho-S6, and phospho-Erk antibodies were purchased from Cell Signaling Technology. Restriction enzymes were purchased from New England BioLabs. Primers, cell culture media and supplements, the TRIzol reagent, Moloney murine leukemia virus (M-MLV) reverse transcriptase, and the Alexa Fluor 488 Tyramide SuperBoost Kit were purchased from Invitrogen. Cas9 protein was purchased from ToolGen. Calcein and Alizarin red S were purchased from Sigma-Aldrich. Anti-Digoxigenin-POD and Anti-Digoxigenin-AP were purchased from Roche.

Generation of *igfbp5a* mutant line using TALEN

TALEN target sites were designed following published criteria (*50*) and are shown in fig. S1A. TALEN constructs were assembled using a Golden Gate cloning strategy following a published protocol (*51*). The assembled plasmids were determined by Stu I and Afl II digestion and confirmed by DNA sequencing.

TALEN-capped mRNA was synthesized by in vitro transcription using T3 polymerase (Ambion mMessage mMachine kit) and injected into embryos at the one-cell stage. After confirming indels using T7E1 assays in a subset of pooled F_0 embryos, the remaining F_0 embryos were raised to adulthood and crossed with wild-type fish. F_1 fish were raised, and caudal fin was severed and genotyped as described below. Positive F_1 fish were subjected to DNA sequencing. The F_1 adult fish were intercrossed, and the progeny were raised and genotyped as described below. To obtain the viable homozygous fish, progeny from the F_1 intercrosses were raised in the 5PPT high [Ca^{2+}] solution in the first month and then transferred into the fish system.

Transient and stable knockout of *igfbp5a* and *5b* genes using CRISPR-Cas9

Two sgRNAs targeting *igfbp5a* exon 1 and two sgRNAs targeting *igfbp5b* exon 1 were designed using the online tool ZiFiT Targeter V4.2 (http://zifit.partners.org/ZiFiT). Their sequences are as follows: *igfbp5a*-sgRNA-1, 5′-GGTGCGGAACGGGTGTCAGGTGG-3′ (sense strand, +114 to +136); *igfbp5a*-sgRNA-2, 5′-GTTCCGCACCGGAGGACACATGG-3′ (anti-sense strand, +123 to +101); *igfbp5b*-sgRNA-1, 5′-GGTGGGCTGTCAGCTAGTGAAGG-3′ (sense strand, +114 to +136); and *igfbp5b*-sgRNA-2, 5′-GTGCGAGCCGTGCGATCAGAAGG-3′ (sense strand, +66 to +88). These sgRNAs were synthesized by in vitro transcription following a published method (*52*). sgRNAs (30 ng/μl) were mixed with Cas9 protein (700 ng/μl) or mRNA (250 ng/μl) and coinjected into *Tg(igfbp5a:GFP)* or wild-type embryos at the one-cell stage. The injected embryos were raised in E3 solution until 72 hpf and transferred to either the regular or low-[Ca^{2+}] solution. NaR cells were quantified at 120 hpf as previously reported (*4*). To generate the *igfbp5b* mutant line, F_0 fish were screened using T7E1 assays with the following primers: *igfbp5b*-gt-F, 5′-AACCCCAACCTGTGTTTTCA-3′; *igfbp5b*-gt-R, 5′-GATACAAACCACCGCACCCA-3′. *igfbp5b* homozygous mutants were obtained following the cross strategy described above.

Genotyping

To isolate genomic DNA, pooled embryos or individual adult caudal fin was incubated in 50 μl of NaOH (50 mM) at 95°C for 10 min, which was neutralized by adding 5 μl of 1 M tris-HCl (pH 8.0). T7E1 assay and HMA were carried out as previously described (*53*). For T7E1 assays, PCR was performed using the following primers: *igfbp5a*-TAL-nF, 5′-GAACGCTGTTCGCTTGAT-3′; *igfbp5a*-TAL-nR, 5′-CGCAGTCCTCGTCCACAT-3′. For HMA assays, PCR was performed using the following primers: *igfbp5a*-HRMA1-F, 5′-GTGGCATTTGTATGGGGACT-3′; *igfbp5a*-HRMA2-R, 5′-AGGTCAAGCAGCATCCGCA-3′.

Individual genotyping was carried out as previously reported (*3*). Briefly, after immunostaining or in situ hybridization analysis, each embryo or larva was washed with 1× phosphate-buffered saline with Tween 20 (PBST) twice and methanol three times. They were air-dried overnight. Then, each embryo or larva was digested in 100 μl SZL buffer [50 mM KCl, 2.5 mM $MgCl_2$, 10 mM tris-HCl (pH 8.3), 0.45% NP-40, 0.45% Tween 20, 0.01% gelatine] containing proteinase K (100 μg/ml) for 1 hour at 60°C. The reaction was stopped by 15-min heat treatment (95°C). After spinning at 10,000 rpm for 1 min, the supernatant was used as template for PCR, followed by HMA assay as previously described (*53*).

Zebrafish larva survival experiments

For survival experiments, embryos or larvae of different genotypes were raised in E3 solution to 72 or 120 hpf. They were then transferred

to the low-[Ca^{2+}] solution. Dead larvae were collected daily and genotyped individually.

Morphology analysis

Body length is defined as the curvilinear distance from the head to the end of caudal tail. Somite number and head-trunk angles were measured manually (*54*, *55*). To visualize the bone morphology, calcein and Alizarin red staining were performed following a published protocol (*56*). For calcein staining, juvenile fish were immersed in the calcein staining solution for 10 min. Then, they were washed three times in E3 solution to remove residual calcein. Images were captured with a stereomicroscope (Leica MZ16F, Leica) equipped with a QImaging QICAM camera (QImaging).

qPCR, whole-mount in situ hybridization, and immunostaining

Total RNA was isolated using TRIzol reagent (Invitrogen). RNA samples were treated with deoxyribonuclease I to remove DNA. One microgram of RNA was reverse-transcribed to single-strand complementary DNA using M-MLV (Promega) and oligo$(dT)_{18}$ primer. Reverse transcription PCR was performed using Taq DNA polymerase (New England BioLabs). qPCR was carried out using SYBR Green (Bio-Rad) on a StepONE PLUS real-time thermocycler (Applied Biosystems). Primers for qPCR used in this study are shown as follows: *igfbp5a*, 5′- GCTGCACGCTCTGCTTTAC-3′ and 5′-AATGGAACCTTGGCCTGAG-3′; *igfbp5b*, 5′-GGGAGTGTGTACGAACGAGAA-3′ and 5′-TCCTGTCACAGTTAGGCAGGTA-3′; *trpv5/6*, 5′-GGACCCTACGTCATTGTGATAC-3′ and 5′- GGTACTGCGGAAGTGCTAAG-3′; β-*actin*, 5′-GATCTGGCATCACACCTTCTAC-3′ and 5′-CCTGGATGGCCACATACAT-3′.

Whole-mount in situ hybridization and immunostaining were performed as previously reported (*3*). For simultaneous in situ hybridization and immunostaining, *mCherry* or *igfbp2b* mRNA was detected using digoxigenin (DIG)–labeled antisense RNA probes (*57*). The *mCherry* signal was detected using anti–DIG-POD antibody (Roche), followed by Alexa 488 Tyramide Signal Amplification (Invitrogen). The *igfbp2b* signal was detected using anti–DIG-AP antibody (Roche), followed by BCIP-NBT (bromochloroindolyl phosphate–nitro blue tetrazolium) staining. After in situ hybridization analysis, the stained larvae were washed in 1× PBST and incubated with phosphorylated Akt or GFP antibody overnight at 4°C. Next, they were stained with a Cy3-conjugated goat anti-rabbit immunoglobulin G antibody (Jackson ImmunoResearch). Fluorescent images were acquired using a Nikon Eclipse E600 Fluorescence Microscope with PMCapture Pro 6 software.

Plasmid and BAC constructs

The construction of the Igfbp5a expression plasmid has been reported (*3*). This plasmid was used as a template to generate Igfbp5a NLS and LBD mutants. For the NLS mutant, the ^{236}KGRK^{239} motif in Igfbp5a C-domain was changed to LDGQ, the corresponding sequence of zebrafish Igfbp1a (*58*) by site-directed mutagenesis (table S1). For the LBD mutant, the sequence ^{86}KPLLL^{92} in Igfbp5a was mutated to NQQQQ (*59*). Human IGFBP5 G223R and IGFBP5 W242* were generated by site-direct mutagenesis (table S1). The resulting Igfbp5a/IGFBP5 DNAs were cloned into the pIRES2-mCherry using the Eco RI and Bam HI sites. The pIRES2-mCherry plasmid was engineered by replacing the DsRed-Express2 cassette in the pIRES2-DsRed-Express2 plasmid with mCherry using the Bst XI and Not I sites. The Igfbp5a/IGFBP5-IRES2-mCherry-KanR cassette DNAs were amplified by PCR using primers listed in table S1. They were inserted into the *igfbp5a* BAC construct (*4*) to replace the *igfbp5a* sequence from the start codon to the end of the first exon through homologous recombination. The resulting BAC DNA was validated by DNA sequencing using primers shown in table S1. The validated *BAC(igfbp5a:Igfbp5a/IGFBP5-mCherry)* DNA constructs were injected into *igfbp5a*$^{-/-}$*;Tg(igfbp5a:GFP)* embryos at the one-cell stage. The embryos were raised in the E3 solution until 72 hpf and then subjected to the low-[Ca^{2+}] challenge test by transferring into low-[Ca^{2+}] solution. Cells coexpressing mCherry and GFP were defined as *igfbp5a/IGFBP5*-expressing NaR cells. They were scored using the scoring system shown in Fig. 5B. A similar cloning strategy was used to generate *BAC(igfbp5a:myr-Akt-mCherry)* plasmids. Constructs were confirmed by DNA sequencing at the University of Michigan DNA Sequencing Core Facility.

Cell culture, transfection, and flow cytometry analysis

Human colorectal carcinoma (LoVo) cells were purchased from American Type Culture Collection and cultured in Dulbecco's modified Eagle's medium/F-12 supplemented with 10% fetal bovine serum, penicillin, and streptomycin in a humidified-air atmosphere incubator containing 5% CO_2 at 37°C. LoVo cells were seeded in six-well plates (Falcon) and transfected with 2 μg of pSuperBP5 or pSuper and 2 μg of pCMV-BP545 or pCMV plasmids using Lipofectamine 2000 (Invitrogen). Twenty-four hours after transfection, the cells were washed and incubated with fresh serum-free medium for 8 hours. IGF2 (400 ng/ml) was then added. Cells were collected after 3 days of IGF2 treatment. Cell cycle analysis was carried out using an Attune Acoustic Focusing Cytometer (Applied Biosystems, Life Technologies), as previously described (*4*). Briefly, a two-parameter dot plot of forward scatter (FSC) versus side scatter was constructed along with a two-parameter dot plot of FL2 [propidium iodide (PI)] area versus FSC area. In addition, a single-parameter FL2 (PI) area histogram was constructed to illustrate relative DNA content in each cell cycle phase.

Statistical analysis

Values are shown as means ± SEM. Statistical significance among experimental groups was determined using unpaired two-tailed *t* test, one-way ANOVA, followed by Tukey's multiple comparison test, log-rank test, or χ^2 test. Statistical significances were accepted at $P < 0.05$ or greater.

SUPPLEMENTARY MATERIALS

www.sciencesignaling.org/cgi/content/full/11/548/eaat2231/DC1

Fig. S1. Generation of *igfbp5a* mutant fish.
Fig. S2. *igfbp5a* mRNA levels in mutant fish.
Fig. S3. Deletion of Igfbp5a does not alter *igfbp5b* expression.
Fig. S4. *igfbp5a Δ4* mutant fish are prone to dying under low Ca^{2+} stress.
Fig. S5. CRISPR-Cas9–mediated transient deletion of Igfbp5a impairs adaptive NaR cell proliferation.
Fig. S6. Expression of IGF and insulin ligand and receptor genes in NaR cells.
Fig. S7. Deletion of Igfbp5a has no effect on phosphorylated Erk signaling.
Table S1. Primers for cloning and sequencing of Igfbp5a, IGFBP5, and their mutants.

REFERENCES AND NOTES

1. P.-P. Hwang, Ion uptake and acid secretion in zebrafish (*Danio rerio*). *J. Exp. Biol.* **212**, 1745–1752 (2009).
2. G. Flik, P. M. Verbost, S. E. Wendelaar Bonga, Calcium transport process in fishes, in *Cellular and Molecular Approaches to Fish Ionic Regulation*, C. M. Wood, T. J. Shuttleworth, Eds. (Academic Press, 1995), pp. 317–342.

3. W. Dai, Y. Bai, L. Hebda, X. Zhong, J. Liu, J. Kao, C. Duan, Calcium deficiency-induced and TRP channel-regulated IGF1R-PI3K-Akt signaling regulates abnormal epithelial cell proliferation. *Cell Death Differ.* **21**, 568–581 (2014).
4. C. Liu, W. Dai, Y. Bai, C. Chi, Y. Xin, G. He, K. Mai, C. Duan, Development of a whole organism platform for phenotype-based analysis of IGF1R-PI3K-Akt-Tor action. *Sci. Rep.* **7**, 1994 (2017).
5. M. M. Beaty, E. Y. Lee, H. P. Glauert, Influence of dietary calcium and vitamin D on colon epithelial cell proliferation and 1,2-dimethylhydrazine-induced colon carcinogenesis in rats fed high fat diets. *J. Nutr.* **123**, 144–152 (1993).
6. S. A. Lamprecht, M. Lipkin, Chemoprevention of colon cancer by calcium, vitamin D and folate: Molecular mechanisms. *Nat. Rev. Cancer* **3**, 601–614 (2003).
7. E. Mokady, B. Schwartz, S. Shany, S. A. Lamprecht, A protective role of dietary vitamin D_3 in rat colon carcinogenesis. *Nutr. Cancer* **38**, 65–73 (2000).
8. C.-L. Tu, Y. Oda, L. Komuves, D. D. Bikle, The role of the calcium-sensing receptor in epidermal differentiation. *Cell Calcium* **35**, 265–273 (2004).
9. R. C. Baxter, IGF binding proteins in cancer: Mechanistic and clinical insights. *Nat. Rev. Cancer* **14**, 329–341 (2014).
10. D. R. Clemmons, W. Busby, J. B. Clarke, A. Parker, C. Duan, T. J. Nam, Modifications of insulin-like growth factor binding proteins and their role in controlling IGF actions. *Endocr. J.* **45**, S1–S8 (1998).
11. D. R. Clemmons, Modifying IGF1 activity: An approach to treat endocrine disorders, atherosclerosis and cancer. *Nat. Rev. Drug Discov.* **6**, 821–833 (2007).
12. C. Duan, Q. Xu, Roles of insulin-like growth factor (IGF) binding proteins in regulating IGF actions. *Gen. Comp. Endocrinol.* **142**, 44–52 (2005).
13. T. L. Wood, L. E. Rogler, M. E. Czick, A. G. P. Schuller, J. E. Pintar, Selective alterations in organ sizes in mice with a targeted disruption of the insulin-like growth factor binding protein-2 gene. *Mol. Endocrinol.* **14**, 1472–1482 (2000).
14. V. E. DeMambro, D. R. Clemmons, L. G. Horton, M. L. Bouxsein, T. L. Wood, W. G. Beamer, E. Canalis, C. J. Rosen, Gender-specific changes in bone turnover and skeletal architecture in *Igfbp-2*-null mice. *Endocrinology* **149**, 2051–2061 (2008).
15. Y. Ning, A. G. P. Schuller, S. Bradshaw, P. Rotwein, T. Ludwig, J. Frystyk, J. E. Pintar, Diminished growth and enhanced glucose metabolism in triple knockout mice containing mutations of insulin-like growth factor binding protein-3, -4, and -5. *Mol. Endocrinol.* **20**, 2173–2186 (2006).
16. M. A. El-Brolosy, D. Y. R. Stainier, Genetic compensation: A phenomenon in search of mechanisms. *PLOS Genet.* **13**, e1006780 (2017).
17. P. Yin, Q. Xu, C. Duan, Paradoxical actions of endogenous and exogenous insulin-like growth factor-binding protein-5 revealed by RNA interference analysis. *J. Biol. Chem.* **279**, 32660–32666 (2004).
18. M. Ding, R. K. Bruick, Y. Yu, Secreted IGFBP5 mediates mTORC1-dependent feedback inhibition of IGF-1 signalling. *Nat. Cell Biol.* **18**, 319–327 (2016).
19. Y. Ning, B. Hoang, A. G. P. Schuller, T. P. Cominski, M.-S. Hsu, T. L. Wood, J. E. Pintar, Delayed mammary gland involution in mice with mutation of the insulin-like growth factor binding protein 5 gene. *Endocrinology* **148**, 2138–2147 (2007).
20. B. Ewen-Campen, S. E. Mohr, Y. Hu, N. Perrimon, Accessing the phenotype gap: Enabling systematic investigation of paralog functional complexity with CRISPR. *Dev. Cell* **43**, 6–9 (2017).
21. Y. Liu, H. Tang, R. Xie, S. Li, X. Liu, H. Lin, Y. Zhang, C. H. K. Cheng, Genetic evidence for multifactorial control of the reproductive axis in zebrafish. *Endocrinology* **158**, 604–611 (2017).
22. H. Tang, Y. Liu, D. Luo, S. Ogawa, Y. Yin, S. Li, Y. Zhang, W. Hu, I. S. Parhar, H. Lin, X. Liu, C. H. K. Cheng, The *kiss/kissr* systems are dispensable for zebrafish reproduction: Evidence from gene knockout studies. *Endocrinology* **156**, 589–599 (2015).
23. J. B. Allard, C. Duan, IGF-binding proteins: Why do they exist and why are there so many? *Front. Endocrinol.* **9**, 117 (2018).
24. F. O. Kok, M. Shin, C.-W. Ni, A. Gupta, A. S. Grosse, A. van Impel, B. C. Kirchmaier, J. Peterson-Maduro, G. Kourkoulis, I. Male, D. F. DeSantis, S. Sheppard-Tindell, L. Ebarasi, C. Betsholtz, S. Schulte-Merker, S. A. Wolfe, N. D. Lawson, Reverse genetic screening reveals poor correlation between morpholino-induced and mutant phenotypes in zebrafish. *Dev. Cell* **32**, 97–108 (2015).
25. A. Rossi, Z. Kontarakis, C. Gerri, H. Nolte, S. Hölper, M. Krüger, D. Y. R. Stainier, Genetic compensation induced by deleterious mutations but not gene knockdowns. *Nature* **524**, 230–233 (2015).
26. P. Zhang, Y. Bai, L. Lu, Y. Li, C. Duan, An oxygen-insensitive Hif-3α isoform inhibits Wnt signaling by destabilizing the nuclear β-catenin complex. *eLife* **5**, e08996 (2016).
27. J. L. Anderson, T. S. Mulligan, M.-C. Shen, H. Wang, C. M. Scahill, F. J. Tan, S. J. Du, E. M. Busch-Nentwich, S. A. Farber, mRNA processing in mutant zebrafish lines generated by chemical and CRISPR-mediated mutagenesis produces unexpected transcripts that escape nonsense-mediated decay. *PLOS Genet.* **13**, e1007105 (2017).
28. D. O. Daza, G. Sundström, C. A. Bergqvist, C. Duan, D. Larhammar, Evolution of the insulin-like growth factor binding protein (IGFBP) family. *Endocrinology* **152**, 2278–2289 (2011).
29. W. Dai, H. Kamei, Y. Zhao, J. Ding, Z. Du, C. Duan, Duplicated zebrafish insulin-like growth factor binding protein-5 genes with split functional domains: Evidence for evolutionarily conserved IGF binding, nuclear localization, and transactivation activity. *FASEB J.* **24**, 2020–2029 (2010).
30. J. Baker, J.-P. Liu, E. J. Robertson, A. Efstratiadis, Role of insulin-like growth factors in embryonic and postnatal growth. *Cell* **75**, 73–82 (1993).
31. J.-P. Liu, J. Baker, A. S. Perkins, E. J. Robertson, A. Efstratiadis, Mice carrying null mutations of the genes encoding insulin-like growth factor I (*Igf-1*) and type 1 IGF receptor (*Igf1r*). *Cell* **75**, 59–72 (1993).
32. M. C. Kiefer, C. Schmid, M. Waldvogel, I. Schläpfer, E. Futo, F. R. Masiarz, K. Green, P. J. Barr, J. Zapf, Characterization of recombinant human insulin-like growth factor binding proteins 4, 5, and 6 produced in yeast. *J. Biol. Chem.* **267**, 12692–12699 (1992).
33. C. A. Conover, M. C. Kiefer, Regulation and biological effect of endogenous insulin-like growth factor binding protein-5 in human osteoblastic cells. *J. Clin. Endocrinol. Metab.* **76**, 1153–1159 (1993).
34. M. R. Schneider, R. Zhou, A. Hoeflich, O. Krebs, J. Schmidt, S. Mohan, E. Wolf, H. Lahm, Insulin-like growth factor-binding protein-5 inhibits growth and induces differentiation of mouse osteosarcoma cells. *Biochem. Biophys. Res. Commun.* **288**, 435–442 (2001).
35. C. M. Bautista, D. J. Baylink, S. Mohan, Isolation of a novel insulin-like growth factor (IGF) binding protein from human bone: A potential candidate for fixing IGF-II in human bone. *Biochem. Biophys. Res. Commun.* **176**, 756–763 (1991).
36. D. L. Andress, R. S. Birnbaum, A novel human insulin-like growth factor binding protein secreted by osteoblast-like cells. *Biochem. Biophys. Res. Commun.* **176**, 213–218 (1991).
37. S. Mohan, Y. Nakao, Y. Honda, E. Landale, U. Leser, C. Dony, K. Lang, D. J. Baylink, Studies on the mechanisms by which insulin-like growth factor (IGF) binding protein-4 (IGFBP-4) and IGFBP-5 modulate IGF actions in bone cells. *J. Biol. Chem.* **270**, 20424–20431 (1995).
38. C. Duan, D. R. Clemmons, Differential expression and biological effects of insulin-like growth factor-binding protein-4 and -5 in vascular smooth muscle cells. *J. Biol. Chem.* **273**, 16836–16842 (1998).
39. H. Ren, P. Yin, C. Duan, IGFBP-5 regulates muscle cell differentiation by binding to IGF-II and switching on the IGF-II auto-regulation loop. *J. Cell Biol.* **182**, 979–991 (2008).
40. Q. Xu, S. Li, Y. Zhao, T. J. Maures, P. Yin, C. Duan, Evidence that IGF binding protein-5 functions as a ligand-independent transcriptional regulator in vascular smooth muscle cells. *Circ. Res.* **94**, e46–e54 (2004).
41. Y. Zhao, P. Yin, L. A. Bach, C. Duan, Several acidic amino acids in the N-domain of insulin-like growth factor-binding protein-5 are important for its transactivation activity. *J. Biol. Chem.* **281**, 14184–14191 (2006).
42. C. Schmid, I. Schlapfer, M. A. Gosteli-Peter, E. R. Froesch, J. Zapf, Effects and fate of human IGF-binding protein-5 in rat osteoblast cultures. *Am. J. Physiol.* **271**, E1029–E1035 (1996).
43. C. A. Conover, C. Oxvig, PAPP-A: A promising therapeutic target for healthy longevity. *Aging Cell* **16**, 205–209 (2017).
44. B. D. Manning, A. Toker, AKT/PKB signaling: Navigating the network. *Cell* **169**, 381–405 (2017).
45. P. Massoner, M. Ladurner-Rennau, I. E. Eder, H. Klocker, Insulin-like growth factors and insulin control a multifunctional signalling network of significant importance in cancer. *Br. J. Cancer* **103**, 1479–1484 (2010).
46. A. Sood, D. McClain, R. Maitra, A. Basu-Mallick, R. Seetharam, A. Kaubisch, L. Rajdev, J. M. Mariadason, K. Tanaka, S. Goel, PTEN gene expression and mutations in the PIK3CA gene as predictors of clinical benefit to anti-epidermal growth factor receptor antibody therapy in patients with KRAS wild-type metastatic colorectal cancer. *Clin. Colorectal Cancer* **11**, 143–150 (2012).
47. C. Zhang, L. Lu, Y. Li, X. Wang, J. Zhou, Y. Liu, P. Fu, M. A. Gallicchio, L. A. Bach, C. Duan, IGF binding protein-6 expression in vascular endothelial cells is induced by hypoxia and plays a negative role in tumor angiogenesis. *Int. J. Cancer* **130**, 2003–2012 (2012).
48. M. Westerfield, *The Zebrafish Book: A Guide for the Laboratory Use of Zebrafish (Danio rerio)* (University of Oregon Press, ed. 4, 2000).
49. C. B. Kimmel, W. W. Ballard, S. R. Kimmel, B. Ullmann, T. F. Schilling, Stages of embryonic development of the zebrafish. *Dev. Dyn.* **203**, 253–310 (1995).
50. V. M. Bedell, Y. Wang, J. M. Campbell, T. L. Poshusta, C. G. Starker, R. G. Krug II, W. Tan, S. G. Penheiter, A. C. Ma, A. Y. H. Leung, S. C. Fahrenkrug, D. F. Carlson, D. F. Voytas, K. J. Clark, J. J. Essner, S. C. Ekker, In vivo genome editing using a high-efficiency TALEN system. *Nature* **491**, 114–118 (2012).
51. T. Cermak, E. L. Doyle, M. Christian, L. Wang, Y. Zhang, C. Schmidt, J. A. Baller, N. V. Somia, A. J. Bogdanove, D. F. Voytas, Efficient design and assembly of custom TALEN and other TAL effector-based constructs for DNA targeting. *Nucleic Acids Res.* **39**, e82 (2011).
52. Y. Shao, Y. Guan, L. Wang, Z. Qiu, M. Liu, Y. Chen, L. Wu, Y. Li, X. Ma, M. Liu, D. Li, CRISPR/Cas-mediated genome editing in the rat via direct injection of one-cell embryos. *Nat. Protoc.* **9**, 2493–2512 (2014).
53. X. Zhu, Y. Xu, S. Yu, L. Lu, M. Ding, J. Cheng, G. Song, X. Gao, L. Yao, D. Fan, S. Meng, X. Zhang, S. Hu, Y. Tian, An efficient genotyping method for genome-modified animals and human cells generated with CRISPR/Cas9 system. *Sci. Rep.* **4**, 6420 (2014).

54. H. Kamei, Y. Ding, S. Kajimura, M. Wells, P. Chiang, C. Duan, Role of IGF signaling in catch-up growth and accelerated temporal development in zebrafish embryos in response to oxygen availability. *Development* **138**, 777–786 (2011).
55. C. Liu, J. Luan, Y. Bai, Y. Li, L. Lu, Y. Liu, F. Hakuno, S.-I. Takahashi, C. Duan, J. Zhou, Aspp2 negatively regulates body growth but not developmental timing by modulating IRS signaling in zebrafish embryos. *Gen. Comp. Endocrinol.* **197**, 82–91 (2014).
56. S. J. Du, V. Frenkel, G. Kindschi, Y. Zohar, Visualizing normal and defective bone development in zebrafish embryos using the fluorescent chromophore calcein. *Dev. Biol.* **238**, 239–246 (2001).
57. S. Zou, H. Kamei, Z. Modi, C. Duan, Zebrafish IGF genes: Gene duplication, conservation and divergence, and novel roles in midline and notochord development. *PLOS ONE* **4**, e7026 (2009).
58. T. J. Maures, C. Duan, Structure, developmental expression, and physiological regulation of zebrafish IGF binding protein-1. *Endocrinology* **143**, 2722–2731 (2002).
59. Y. Zhong, L. Lu, J. Zhou, Y. Li, Y. Liu, D. R. Clemmons, C. Duan, IGF binding protein 3 exerts its ligand-independent action by antagonizing BMP in zebrafish embryos. *J. Cell Sci.* **124**, 1925–1935 (2011).

Acknowledgments: We thank J. Allard for critically reading and editing of the initial draft of the manuscript. This work was supported by NSF grant IOS-1557850 and MCube2.0 Project U0496246 to C.D. **Author contributions:** C.D. conceived the study. C.D., C.L., and Y.X. designed the experiments and wrote the paper. C.L., Y.X., Y.B., and G.L. performed the experiments and carried out the analysis. G.H. and K.M. analyzed the data. All authors have contributed to and approved the final manuscript. **Competing interests:** The authors declare that they have no competing interests. **Data and materials availability:** All data needed to evaluate the conclusions in the paper are present in the paper or the Supplementary Materials.

Submitted 5 February 2018
Accepted 30 August 2018
Published 18 September 2018
10.1126/scisignal.aat2231

Citation: C. Liu, Y. Xin, Y. Bai, G. Lewin, G. He, K. Mai, C. Duan, Ca^{2+} concentration–dependent premature death of *igfbp5a*$^{-/-}$ fish reveals a critical role of IGF signaling in adaptive epithelial growth. *Sci. Signal.* **11**, eaat2231 (2018).

Science Signaling

Ca^{2+} concentration–dependent premature death of *igfbp5a*$^{-/-}$ fish reveals a critical role of IGF signaling in adaptive epithelial growth

Chengdong Liu, Yi Xin, Yan Bai, Grant Lewin, Gen He, Kangsen Mai and Cunming Duan

Sci. Signal. **11** (548), eaat2231.
DOI: 10.1126/scisignal.aat2231

Stressing out about low Ca^{2+}

Under low Ca^{2+} conditions, an epithelial cell population in zebrafish known as NaR cells proliferate so that they can take up more Ca^{2+}. Liu *et al*. found that Igf-binding protein 5A (Igfbp5a) was required for this adaptive proliferation and for survival under low Ca^{2+} conditions. The defect in NaR adaptive proliferation in *igfbp5a*$^{-/-}$ zebrafish was rescued by expression of wild-type human or zebrafish IGFBP5 but not two cancer-associated IGFBP5 mutants. Mice deficient in the various IGFBPs lack obvious phenotypes, and these results reveal the importance of using the appropriate physiological conditions to determine the function of IGFBPs.

Science Signaling (ISSN 1937-9145) is published by the American Association for the Advancement of Science, 1200 New York Avenue NW, Washington, DC 20005. The title *Science Signaling* is a registered trademark of AAAS.